Regulation of Phosphoglucose Isomerase/Autocrine Motility Factor Activities by the Poly(ADP-Ribose) Polymerase Family-14

Takashi Yanagawa,[1,2] Tatsuyoshi Funasaka,[1] Soichi Tsutsumi,[3] Huankai Hu,[1] Hideomi Watanabe,[4] and Avraham Raz[1]

[1]Tumor Progression and Metastasis Program, Karmanos Cancer Institute, School of Medicine, Wayne State University, Detroit, Michigan; Departments of [2]Orthopaedic Surgery and [3]General Surgical Science (Surgery I), School of Medicine, and [4]Department of Physical Therapy, School of Health Science, Gunma University, Gunma, Japan

Abstract

Phosphoglucose isomerase (PGI; EC 5.3.1.9) is a ubiquitous cytosolic enzyme essential for glycolysis and gluconeogenesis. PGI is a multifunctional dimeric protein that extracellularly acts as a cytokine [autocrine motility factor (AMF)] eliciting mitogenic, motogenic, and differentiation functions through binding to its cell surface receptor gp78/AMF receptor (AMFR). AMFR contains a seven-transmembrane domain with RING-H2 and leucine zipper motifs showing ubiquitin protein ligase (E3) activity and is exposed on the endoplasmic reticulum surface. Augmented expressions of both PGI/AMF and AMFR have been implicated in tumor progression and metastasis, and an intracellular binding partner of PGI/AMF is expected to regulate in part its diverse biological functions. Thus, we screened a cDNA library using a yeast two-hybrid system to search for interacting protein(s) and report on the finding of poly(ADP-ribose) polymerase-14 (PARP-14) to be a binding partner with PGI/AMF. PARP-14–PGI/AMF interaction was confirmed by coimmunoprecipitation and immunolocalization. We also report that PGI/AMF degradation is mainly regulated by the ubiquitin-lysosome system and RNA interference experiments revealed that PARP-14 inhibits PGI/AMF ubiquitination, thus contributing to its stabilization and secretion. This newly characterized PARP-14 protein should assist in understanding the regulation of PGI/AMF intracellular function(s) and may provide a new therapeutic target for inhibition of PGI/AMF inducing tumor cell migration and invasion during metastasis. [Cancer Res 2007;67(18):8682–9]

Introduction

Phosphoglucose isomerase (PGI) is a ubiquitous multifunctional protein that intracellularly catalyzes the interconversion of glucose 6-phosphate and fructose 6-phosphate (the second step of the Embden-Meyerhof glycolytic pathway; ref. 1); plays important roles in angiogenesis, metastasis, and vessel leakiness; and extracellularly behaves as a cytokine, identified as autocrine motility factor (AMF; refs. 2–4). Other functions of PGI/AMF are as T cell lymphokine (e.g., neuroleukin) that supports the survival of spinal and sensory neurons (5), maturation factor that differentiates myeloid leukemic cells to terminal monocytic cells (6), sperm antigen-36 (7), and myofibril-bound serine proteinase inhibitor (8). In addition, PGI/AMF is an antigen of arthritis diseases (9) and is detected in rheumatoid synovial fluid (10). Reduction in expression or activity of PGI/AMF causes hereditary nonspherocytic hemolytic anemia diseases in human (11, 12). Secreted AMF promotes cancer cell invasion and metastasis by stimulating cell motility via an autocrine manner after binding to its 78 kDa seven-transmembrane glycoprotein receptor, gp78/AMFR (13). AMF in the serum or urine can be a tumor marker predicting patients' prognosis with cancer (14–16). The signaling pathways downstream of AMFR include protein kinase CK2 (17), Rho family regulators, the rho GDP dissociation inhibitor β, and kinesin motor 3A, and is implicated in epithelial-mesenchymal transition by down-regulation of E-cadherin expression through the up-regulation of its transcription suppressor (e.g., Snail; refs. 18, 19). We cloned the human and the mouse *gp78/AMFR* genes that were found to encode a novel conserved seven-transmembrane protein harboring a RING-H2 motif and a leucine zipper motif (20). Subsequently, gp78 was also found to be an endoplasmic reticulum membrane–anchored ubiquitin ligase (E3) involved in unubiquitination of endoplasmic reticulum proteins (21) and to have a structural similarity to the yeast ERAD E3 ligase Hrd1p/Der3p protein. More recently, it has been shown that gp78 and a specific E2, Ube2g2, are both critically important for endoplasmic reticulum–associated degradation (ERAD) and suggested that gp78-mediated ubiquitination is an early step in ERAD that precedes dislocation of substrates from the endoplasmic reticulum (22). It was further proposed that it ubiquitinates a misfolded substrate while it is being retrotranslated, and p97, mPNGase, and mHR23B form a complex bridging the endoplasmic reticulum and the proteasome (23).

Based on the above and the fact that AMF/PGI undergoes posttranslation modification by CK2 protein kinase phosphorylation (17), that insulin-like growth factor binding protein-3 regulates its activity (24), and that its expression in human breast carcinoma cells is down-regulated by anti–epidermal growth factor receptor antibodies (25), we examined the possible existence of an AMF/PGI binding partner(s). Thus, we have used the CytoTrap yeast two-hybrid screening system and report on the identification of a novel-binding-partner belonging to the poly(ADP-ribose)polymerase (PARP) family (e.g., PARP-14).

Materials and Methods

Cells and monolayer culture conditions. Human fibrosarcoma cell line HT-1080 and human skin fibroblast cell line Hs68 were obtained from American Type Culture Collection (ATCC) and grown in DMEM. Human osteosarcoma cell lines HuO9 and NOS were kindly provided by Dr. Hotta (Niigata University, Niigata, Japan) and colon cancer cell line HT-29 and MKN 45 were purchased from ATCC and Riken Gene Bank, respectively, and grown in RPMI 1640. Human umbilical vein endothelial cells were

Note: Supplementary data for this article are available at Cancer Research Online (http://cancerres.aacrjournals.org/).

Requests for reprints: Avraham Raz, Tumor Progression and Metastasis Program, Karmanos Cancer Institute, School of Medicine, Wayne State University, 110 East Warren Avenue, Detroit, MI 48201. Phone: 313-833-0960; Fax: 313-831-7518; E-mail: raza@karmanos.org.

doi:10.1158/0008-5472.CAN-07-1586

purchased from Cambrex and cultured in endothelial cell basal medium-2 (Cambrex). All cell lines were supplemented with 10% heat-inactivated fetal bovine serum and maintained at 37°C in a humidified atmosphere of 5% CO_2 and 95% air.

cDNA library screening using the CytoTrap system. To find the proteins interacting with PGI/AMF, cDNA library screening was done using the CytoTrap two-hybrid system (Stratagene) according to the instruction manual. Briefly, mouse *pgi/amf* gene that had been generated as previously reported (18) was inserted into pSos vector to produce human son of sevenless (hSos) protein fused with mouse PGI/AMF, which was used as a bait protein. cDNA library originated from mouse smooth muscle and inserted into pMyr vector that contains DNA encoding the myristylation membrane localization signal (Myr) was also purchased from Stratagene. The temperature-sensitive phenotype of the cell division cycle 25H (cdc25H) yeast host strain, which can grow at 25°C but not at 37°C, was cotransformed with bait plasmid and pMyr plasmid including cDNA library extracted from 3×10^4 colonies. Transformed yeast cells were cultured on synthetic glucose minimal medium [SD/glucose(−UL)] or synthetic galactose minimal medium [SD/galactose(−UL)] plates composed of 0.17% yeast nitrogen, 0.5% ammonium sulfate and 2% dextrose or 0.17% yeast nitrogen, 0.5% ammonium sulfate, 2% galactose and 1% raffinose, respectively, and supplemented with amino acids without uracil and leucin.

The clone that was able to survive at 37°C on the agar plate with galactose but not with glucose was selected as a putative interactor candidate. pMyr cDNA plasmid DNA was isolated from the selected clone using YEASTMAKER Yeast Plasmid Isolation kit (BD Biosciences). The isolated plasmid was used for transformation again and the transformed yeast was verified to survive under the same restrictive condition. pSos V-maf musculoaponeurotic fibrosarcoma oncogene homologue B (MAFB) + pMyr MAFB and pSos MAFB + pMyr Lamin C plasmids were used for cotransformation as a positive and negative control, respectively (26, 27). The plasmid selected through the screening was sequenced and the homology search was done with National Center for Biotechnology Information BLAST Sequence Homology Search server.[5]

Immunoblotting of hSos and PGI/AMF fusion protein expressed in yeasts. After transformation with the plasmid, the yeast cells were verified to express a bait protein. Increased yeast cells were resuspended with 1 mL of distilled H_2O and 150 μL of 7.5% β-mercaptoethanol in 1.85 mol/L NaOH was added to the cell suspension. Samples were placed on ice for 10 min after addition of 55% trichloroacetic acid in water. The proteins were extracted by centrifugation, resuspended in 300 μL of SU buffer composed of 5% SDS, 8 mol/L urea, 125 mmol/L Tris, 0.1 mmol/L EDTA, 0.005% bromophenol blue, 15 mg/mL DTT, heated at 65°C for 3 min, loaded to SDS-PAGE, and transferred to a polyvinylidene difluoride (PVDF) membrane. The fusion protein was detected with anti-Sos1 antibody (BD Biosciences).

Immunoprecipitation assay. Polyclonal antibody specific to PARP-14 was generated by Biosource based on the sequence CARDEIEAMIKRVRLAKE. The HT-1080 cells seeded on 10-cm dishes were washed with PBS thrice and incubated with 2 mmol/L dithio-bis(succinimidyl propionate) (DSP) cross-linker (Pierce), in PBS for 30 min, and then the reactions were quenched with 50 mmol/L Tris for 15 min. Cells were lysed in radioimmunoprecipitation assay (RIPA) buffer (20 mmol/L Tris, 150 mmol/L NaCl, 1% Triton X-100, 1% NP40, 10 mmol/L EDTA, and 25 mmol/L sodium deoxycholate) and centrifuged at 15,000 × *g* for 5 min. The supernatants were pretreated with Protein G Sepharose (Amersham Biosciences) and used as the cell extracts. The cell extracts were incubated with anti-human PGI/AMF polyclonal antibody or control rabbit IgG for 1 h at 4°C, followed by 1-h incubation with Protein G Sepharose. The beads were washed extensively with washing buffer (50 mmol/L Tris, 150 mmol/L NaCl, and 0.05% Triton X-100) and incubated with sample buffer, including DTT, to cleave DSP. Samples were subjected to SDS-PAGE and transferred to a PVDF membrane, which was probed with the polyclonal antibody specific to PARP-14 and the immunoreactive protein was detected.

Confocal immunofluorescence microscopy. HT-1080 cells were plated on glass coverslips coated with bovine serum albumin (BSA). After 24 h, cells were fixed with chilled methanol for 4 min and blocked with 3% BSA in PBS for 30 min. After the blocking step, anti–PARP-14 polyclonal antibody and anti–PGI/AMF monoclonal antibody (Pfizer) were added at 1:100 and 1:10 dilution, respectively, and the mixture was incubated for 1 h. Secondary antibodies [FITC-conjugated goat anti-rabbit IgG (Zymed) and Texas red–conjugated anti-mouse IgG (ICN)] were added at a 1:100 dilution, followed by 1-h incubation. The coverslips bearing the stained cells were mounted using Prolong Antifade mounting medium (Molecular Probes) for viewing and photomicrography.

For visualization of mitochondria, cells were stained for 45 min with 100 nmol/L MitoTracker Red (Molecular Probes) and fixed in a solution of 3.7% paraformaldehyde in PBS for 15 min. Fixed cells were permeabilized for 10 min in ice-cold acetone, preincubated in blocking solution (3% BSA in PBS), and then incubated for 1 h with anti–PGI/AMF primary antibodies. The cells were then washed, probed with a fluorescence-conjugated secondary antibody, and mounted for microscopic observation.

For confocal immunofluorescence microscopy analysis, the stained cells were observed using Zeiss Laser Scanning Microscope 310 (Zeiss). The cells were scanned by dual excitation of fluorescein (green) and Texas red (red) fluorescence. Areas of green and red overlapping fluorescence were represented by a yellow signal.

RNA interference against PARP-14. The small interfering RNA (siRNA) sense sequences against PARP-14 and firefly (*Photinus pyralis*) luciferase (GL3) as a control were 5′-CUAGUGCAGAUGUGUAUAATT-3′ designed by Dharmacon si*DESIGN* Center (Dharmacon) and 5′-CUUACGCUGAGUACUUCGATT-3′ as previously reported, respectively (28). HT-1080 cells were transfected with siRNA using LipofectAMINE 2000 according to the manufacturer's instruction (Invitrogen). PARP-14 expression in transfected cells was examined with immunoblotting as mentioned above.

Detection of PGI/AMF expression under PARP-14–suppressed condition. Conditioned medium of confluent HT-1080 cells was replaced to serum-free medium 24 h after transfection with siRNA against PARP-14, and 12 h later cells and conditioned medium were collected. Equal amounts of protein of conditioned medium concentrated with Ultrafree-0.5 Centrifugal Filter Units (Millipore) and cell lysate in RIPA buffer were examined with immunoblotting using anti–PGI/AMF monoclonal antibody.

Conditions of PCR reaction. Total RNA was isolated from siRNA-transfected HT-1080 cells using TRIzol (Invitrogen). A measure of 3 μg of total RNA was used as a template for cDNA synthesis. The products of reverse transcription reactions were used for PCR. The housekeeping gene *human ribosomal protein S14* (*hRPS14*) was used as a control. The numbers of amplification cycles for *pgi/amf, parp-14*, and *hrps14* genes were 25, 35, and 25 times, respectively, which were selected to allow linear amplification of the cDNA under study. For quantitative evaluation of the amplified product, PCR with 20 to 40 cycles was preliminarily done. The primer sequences and their respective PCR fragment lengths were as follows: PGI/AMF, 5′-AATGCAGAGACGGCGAAGGAG-3′ and 5′-ACGAGAAGAGAAAGGGGAGTC-3′ (1,066 bp); PARP-14, 5′-ATGGCCACAAAACTCGACTT-3′ and ATTATGAAAGGGAAGCTGAAGAAAG-3′ (4,719 bp); hRPS14, 5′-GGCAGACCGAGATGAATCCTC-3′ and 5′-CAGGTCCAGGGGTCTTGGTCC-3′ (143 bp). Amplified DNA samples were electrophoresed on 1% agarose gels and photographed.

Measurement of PGI enzymatic activity. *In vivo* PGI enzymatic activity of siRNA-transfected cells was measured as previously described (29). Briefly, 48 h after transfection with siRNA, cells were lysed in RIPA buffer and 50 μg/protein of each sample were added to the reaction mixture that consists of 0.1 mol/L Tris (pH 8.5), 4.0 mmol/L fructose-6-phosphate, 0.5 mmol/L NADP, and 1 unit/mL of glucose 6-phosphate dehydrogenase; its enzymatic activity was immediately monitored at $A_{340\ nm}$ for 10 min with a spectrophotometer (Shimadzu).

Immunoblotting of PARP-14 in normal and tumor cell lines. HT-1080 and Hs68 cells expanded on 10-cm dishes were lysed in RIPA buffer. After cell lysates were centrifuged, supernatants were subjected to

[5] http://www.ncbi.nlm.nih.gov/BLAST

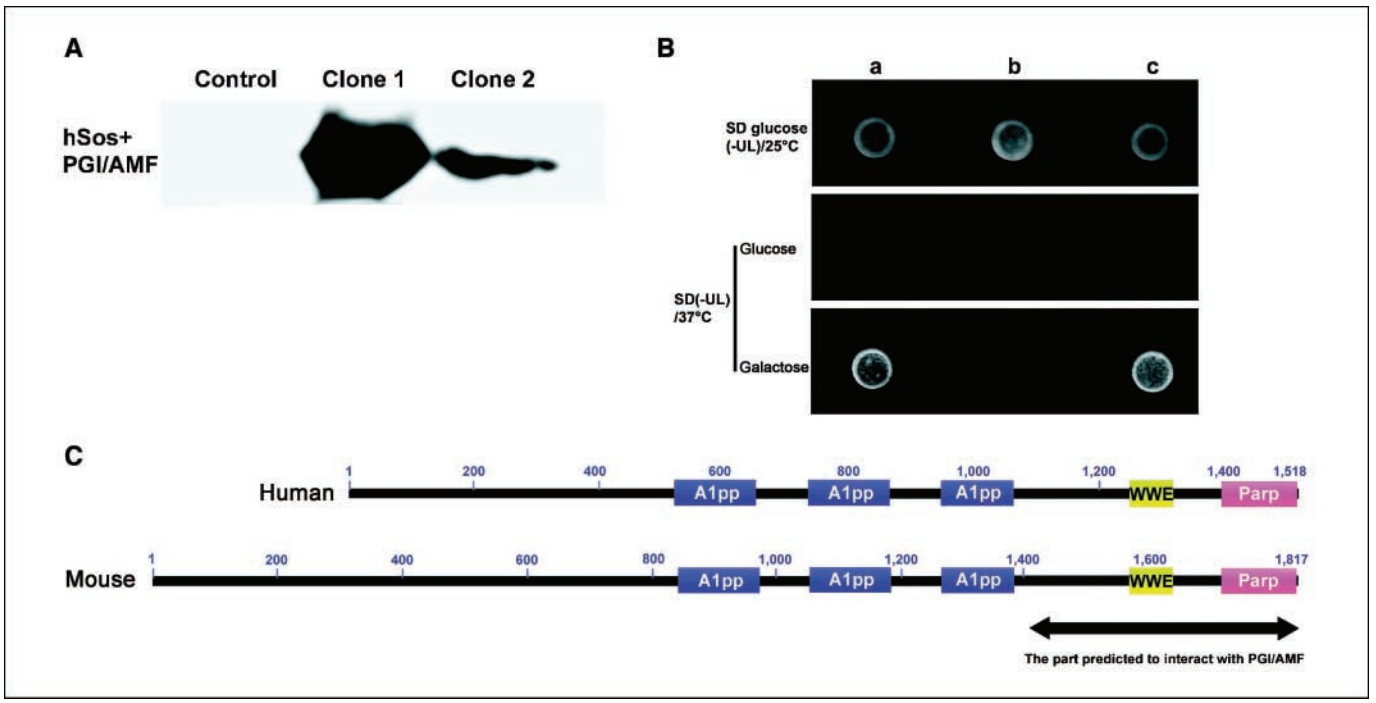

Figure 1. Screening of cDNA library to find the proteins interacting with PGI/AMF using the CytoTrap two-hybrid system. *A,* the expression of hSos and PGI/AMF fusion protein. Yeast cells were transfected with pSos vector including mouse *pgi/amf* gene or null vector (*Control*). The expression of fusion protein examined in two clones was confirmed by Western blotting. *B,* verification of the interaction between the candidate and PGI/AMF. The plasmid was isolated from the clone selected through the two-hybrid screening and the specificity of the interaction was verified by cotransformation with bait and isolated plasmids (*a*). Transformed yeast cells were cultured on SD/glucose(−UL) or SD/galactose(−UL) agar plates. pSos MAFB + pMyr Lamin C (*b*) and pSos MAFB + pMyr MAFB (*c*) plasmids were used for cotransformation as negative and positive controls, respectively. The interaction between the bait and target proteins allow yeast cells to survive at 37°C on SD/galactose(−UL) agar plate but not on SD/glucose(−UL). *C,* structure of PARP-14. Domain structure of human and mouse PARP-14. PARP-14 consists of three A1pp domains in the NH_2 terminus, and one WWE domain and PARP-1 catalytic domain in the COOH terminus. The cDNA we cloned included the WWE and PARP catalytic domains; therefore, they were predicted to interact with PGI/AMF.

SDS-PAGE and transferred to a PVDF membrane, which was probed with anti–PARP-14 polyclonal antibody or anti–PGI/AMF monoclonal antibody, and immunoreactive protein was detected. Conditioned medium was also collected as mentioned above and probed with anti–PGI/AMF monoclonal antibody.

Detection of PGI/AMF ubiquitination. To determine whether PGI/AMF is degraded by ubiquitin-proteasome or ubiquitin-dependent lysosomal system, HT-1080 cells were treated with 20 μmol/L lactacystin (Sigma) and 20 μmol/L MG132 (Wako), specific proteasome inhibitors, or 100 μmol/L chloroquine (Sigma) and 20 mmol/L ammonium chloride

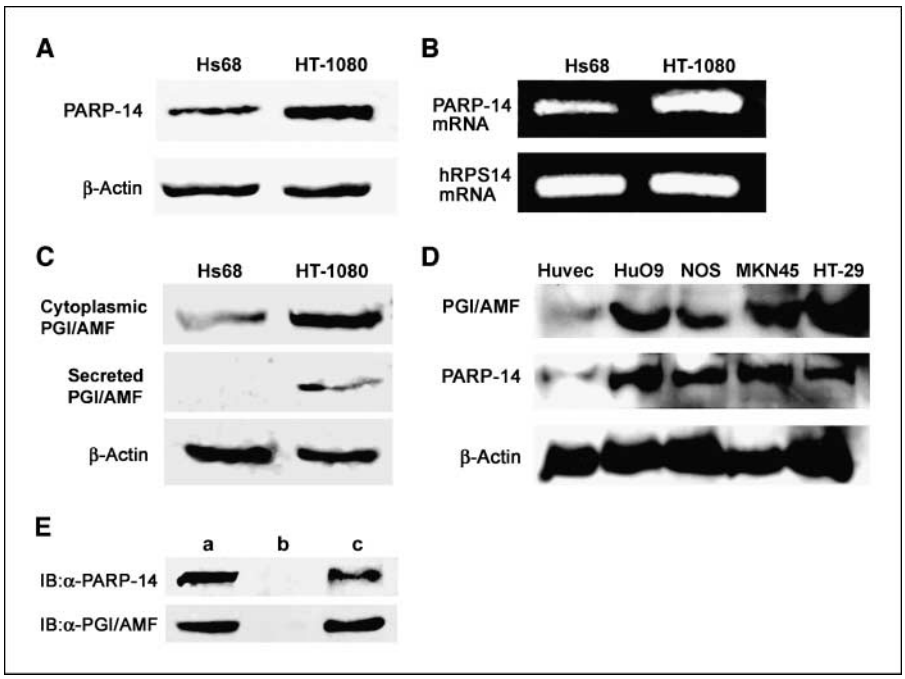

Figure 2. Expression of PARP-14 and PGI/AMF in normal and tumor cell lines. *A* and *B,* expression of PARP-14. HT-1080 and Hs68 cells expanded on 10-cm dishes were lysed in RIPA buffer and analyzed with Western blotting. At the same time, total RNA was also isolated from the cells using TRIzol. A measure of 3 μg of total RNA was used as a template for cDNA synthesis. The products of reverse transcription reactions were used for PCR. HT-1080 cells showed higher PARP-14 expression than Hs68 cells did at protein (*A*) and mRNA levels (*B*). *C,* expression and secretion of PGI/AMF. PGI/AMF protein was detected with anti–PGI/AMF monoclonal antibody. HT-1080 cells intracellularly expressed and secreted more PGI/AMF than Hs68 cells. *D,* expressions of PGI/AMF and PARP-14 in various cell lines. Malignant cells showed higher PGI/AMF and PARP-14 expressions than normal cells at protein level. *Huvec,* human umbilical vein endothelial cells. *E,* immunoprecipitation assay. Lysate of HT-1080 cells was immunoprecipitated with anti–PGI/AMF polyclonal antibody or preimmunized rabbit IgG, subjected to SDS-PAGE, and transferred to a PVDF membrane; then, precipitated proteins were detected with anti–PARP-14 or anti–PGI/AMF polyclonal antibody. Anti–PARP-14 antibody could not immunoprecipitate proteins, indicating it may not be suitable for immunoprecipitation. *Lane a,* whole-cell lysate; *lane b,* preimmunized rabbit IgG; *lane c,* anti–PGI/AMF polyclonal antibody. *IB,* immunoblotting.

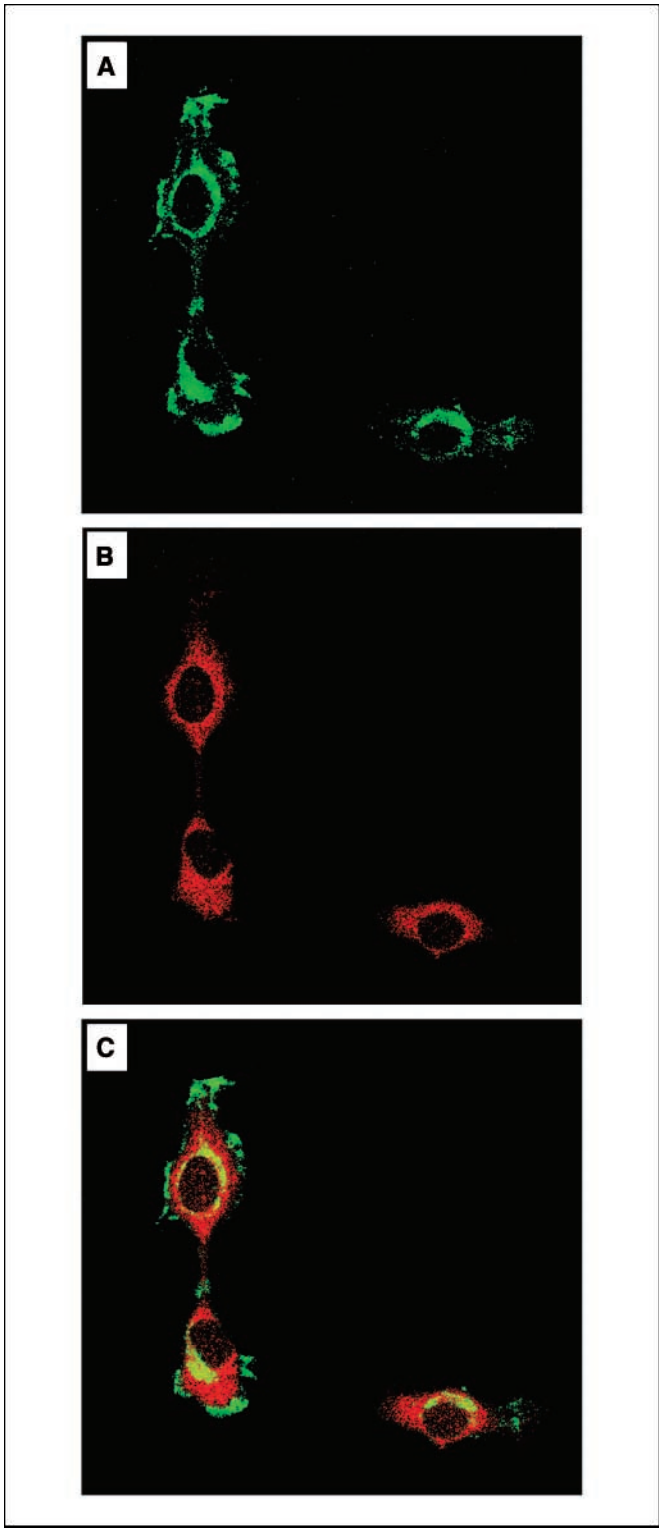

Figure 3. Distribution of PARP-14 and PGI/AMF. HT-1080 cells were plated on glass coverslides coated with BSA. After 24 h, cells were fixed with chilled methanol for 4 min and blocked with 3% BSA in PBS for 30 min. *A,* PARP-14 was detected with anti–PARP-14 polyclonal antibody and FITC-conjugated secondary antibody under confocal immunofluorescence microscopy and found to predominantly localize at the perinuclear region and slightly at the peripheral region of the cells. *B,* PGI/AMF was probed with anti–PGI/AMF monoclonal antibody and Texas red–conjugated secondary antibody and found to be distributed throughout the cytoplasm. *C,* confocal immunofluorescence microscopy analysis revealed that PARP-14 colocalized with PGI/AMF only at the perinuclear region.

(Sigma), lysosome inhibitor, for 5 h, and PGI/AMF protein levels in cytoplasm and conditioned medium were determined by immunoblotting. To examine ubiquitination of PGI/AMF, HT-1080 cells treated with lactacystin or chloroquine were lysed in RIPA buffer and centrifuged, and supernatants were pretreated with Protein G Sepharose and incubated with anti–PGI/AMF monoclonal antibody or anti-ubiquitin polyclonal antibody (Novus Biologicals, Inc.) for 1 h followed by 1-h incubation with Protein G Sepharose. Samples were examined with immunoblotting using anti-ubiquitin polyclonal antibody or PGI/AMF monoclonal antibody.

Transwell motility assays. The directional motility was assayed using 6.5-mm Transwell supports with 8.0-μm pore polycarbonate membrane inserts (Corning Life Sciences). One hundred microliters of cell suspension (1×10^5 cells/mL) were added to the upper compartment, and 600 μL of DMEM with 10% fetal bovine serum was added to the lower compartment. After a 6-h incubation with 100 pg/mL recombinant PGI/AMF proteins at 37°C, the membranes were fixed with 70% ethanol for 1 h, stained with 0.4% trypan blue, and washed with distilled water. The cells that invaded through the membrane were counted after the cells on the upper surface of the membrane were swiped with cotton swabs.

Results

Isolation of cDNA encoding a protein interacting with PGI/AMF. To search for PGI/AMF–interacting protein(s), we have used the CytoTrap two-hybrid system based on generating two types of fusion proteins whose interaction in the yeast cytoplasm activates the Ras-signaling pathway, inducing cell growth. After transformation and screening, two yeast clones were selected, both of which were confirmed to express both hSos and mouse PGI/AMF (bait) fusion proteins (Fig. 1*A*). Next, the plasmid was isolated and the specificity of the interaction was verified by cotransformation with bait and isolated plasmids (Fig. 1*B*).

The isolated plasmid was sequenced, and after a homology search we found that the sequence was identical to a portion of the mouse KIAA1268 (Genbank accession no. XM_488522) with a single base pair difference (the 4,865th base pair) that changes one amino acid (the 1,609th amino acid), including the WWE and PARP catalytic domains (Fig. 1*C*). The reported mouse KIAA1268 sequence is considered to be an NH_2-terminal truncated protein with 65% of identity with that of human PARP-14 (Genbank accession no. NM_017554), which is an alias of human KIAA1268 (Fig. 1*C*). Next, an anti-human PARP-14 polyclonal antibody was generated using a synthetic peptide adding cysteine at the NH_2 terminus (CARDEIEAMIKRVRLAKE) as an antigen. Of note, this sequence is identical to that of mouse except for three amino acids (ARDEIEGMIKSIRLAKE). From the Expasy web site, [6] the theoretical molecular weight of the human PARP-14 consisting of 1,518 amino acids polypeptide is ~170.6 kDa. Next, we examined the expression of PARP-14 by human lung-derived tumor and normal cells, HT-1080 and Hs68 cells, respectively. Anti–PARP-14 antibodies detected the expression of an ~158 kDa protein in both cell extracts although the HT-1080 cells expressed an ~2-fold higher level compared with Hs68 cells, which was a reflection of a higher mRNA level of 4,719 bp (Fig. 2*A* and *B*). The total and the secreted PGI/AMF protein levels are depicted in Fig. 2*C*. This confirms previous results showing that all cells expressed PARP-14 protein (Fig. 2*D*) and that tumor cells express a higher level of the protein than normal cell which fail to secrete it (2).

[6] http://au.expasy.org/

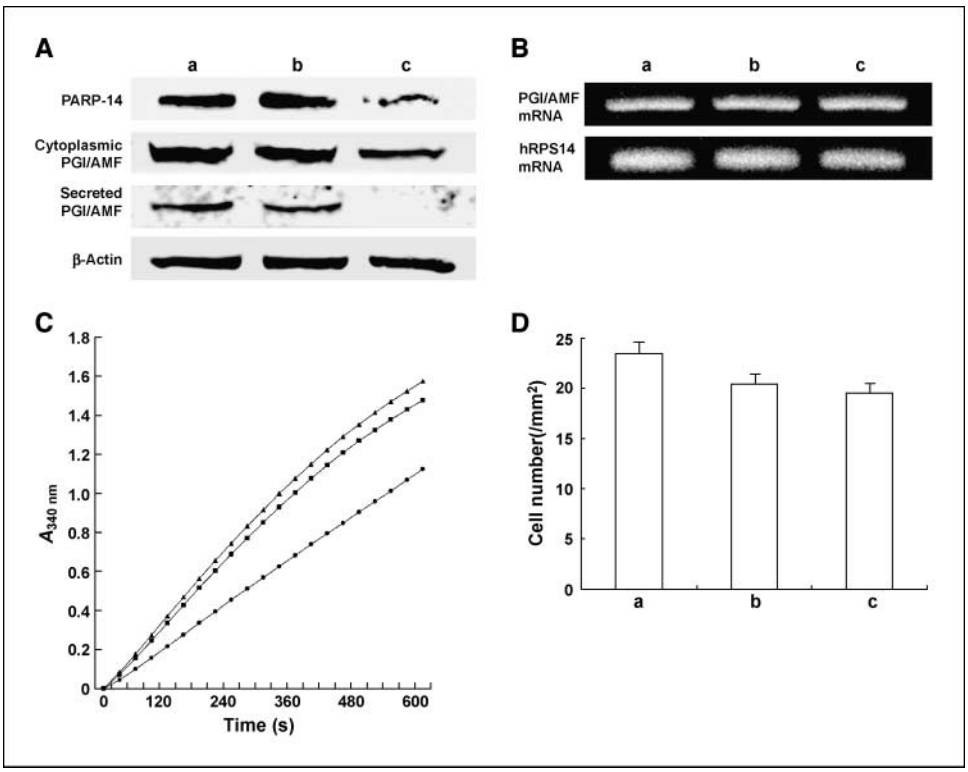

Figure 4. Effect of PARP-14 on characters of PGI/AMF. *A* and *B,* the expressions of PGI/AMF and PARP-14 in the cells transfected with siRNA against PARP-14. Two days after transfection, cell lysates and conditioned medium were examined. The PARP-14 expression of the cells transfected with siRNA against PARP-14 reduced to 30% or less of that of controls (*A*). There were no differences in morphology and viability among the cells. The cells transfected with siRNA against PARP-14 expressed an equal amount of PGI/AMF to control cells at mRNA level (*B*); however, they expressed only ~60% of PGI/AMF than control cells and secreted little AMF into conditioned medium (*A*). *a,* parental cells; *b,* HT-1080 cells transfected with GL3 siRNA; *c,* HT-1080 cells transfected with PARP-14 siRNA. *C,* PGI enzymatic activity. Two days after transfection with siRNA, cells were lysed in RIPA buffer and 50 μg/protein of each sample were added to the reaction mixture and immediately its enzymatic activity was monitored at $A_{340\ nm}$ for 10 min with a spectrophotometer. The enzymatic activity of HT-1080 cells transfected with siRNA against PARP-14 diminished to <65% of that of controls. ▲, parental cells; ■, HT-1080 cells transfected with GL3 siRNA; •, HT-1080 cells transfected with PARP-14 siRNA. *D,* AMF cytokine activity. Suppression of PARP-14 did not down-regulate cell motility. *a,* parental cells; *b,* HT-1080 cells transfected with GL3 siRNA; *c,* HT-1080 cells transfected with PARP-14 siRNA.

To explore whether *in vivo* PGI/AMF interacts with PARP-14, the lysates of HT-1080 cells prepared from monolayer cultures were immunoprecipitated with either anti–PGI/AMF polyclonal antibodies or preimmunized rabbit IgG and blotted with anti–PARP-14 or anti–PGI/AMF antibodies (Fig. 2*E*). The results clearly show that PARP-14 coprecipitated with PGI/AMF, suggesting that the two are complexed *in vivo*. Next, we confirmed that PARP-14–PGI/AMF are indeed colocalized *in vivo* in HT-1080 cells by immunofluorescence analysis (Fig. 3) using confocal microscopy. PARP-14 was found to predominantly localize at the perinuclear region and slightly at the peripheral region of the cells (Fig. 3*A*), whereas PGI/AMF was distributed throughout the cytoplasm (Fig. 3*B*) and colocalization was readily observed mainly in the perinuclear region (Fig. 3*C*). On the other hand, the endogenous PGI/AMF expression did not overlap with the mitochondria pattern in the cytoplasm (Supplementary Fig. S1).

Effect of PARP-14 on PGI/AMF. If indeed PARP-14 is a binding partner of PGI/AMF, does it affect expression, secretion, and/or enzymatic activity? To address this, HT-1080 cells were transfected with siRNA against PARP-14, and 2 days after transfection cell lysates and conditioned medium were tested for protein expression levels. Initially, we established the potency of the siRNA against PARP-14; the treatment significantly reduced its expression level (Fig. 4*A*; parental cells: 1.00, mock cells: 1.11, PARP-14 siRNA cells: 0.32). Of note, the PARP-14 siRNA also markedly inhibited the expression level of PGI/AMF (parental cells: 1.00, mock cells: 0.93, PARP-14 siRNA cells: 0.56) compared with that of the control cells and led to elimination of its secretion (Fig. 4*A*). It should be noted that no change in cell morphology or viability could be detected between the transfectants and the control cells (not shown). Furthermore, the inhibition of PGI/AMF expression and secretion was not due to inhibition at the level of transcription, as the cells transfected with siRNA against PARP-14 expressed similar amounts of PGI/AMF mRNA as the control cells (Fig. 4*B*). The reduction in the level of PGI/AMF protein expression was also reflected in a comparable reduction of its total cellular enzymatic activity, calculated with the slope of the linear phase of the graph (Fig. 4*C*). However, unexpectedly, suppression of PARP-14 did not affect cell motility (Fig. 4*D*).

Because it is now established that the level of PGI/AMF secretion relates to its level of expression (2, 18, 30) and the above results show that suppression of PARP-14 expression leads to a reduced PGI/AMF expression/secretion without a detectable change in PGI/AMF transcription (Fig. 4*B*), we examined whether PARP-14 affects the stability of the PGI/AMF protein, which compelled us to examine the degradation mechanisms of PGI/AMF. There are two major protein degradation pathways, the ubiquitin-proteasome and ubiquitin-lysosome systems. It was reported that polyubiquitin chains target proteins for specific degradation by proteasome (31) and monoubiquitination serves as a signal to regulate the activity

of components of the endosome/lysosome pathway (32). To explore these possibilities, we initially treated HT-1080 cells with the lysosome inhibitors, which up-regulated PGI/AMF accumulation (Fig. 5*A*; chloroquine: 1.61 ratio to control, ammonium chloride: 2.52). Next, we incubated HT-1080 cells with proteasome inhibitors and found that PGI/AMF did not accumulate (Fig. 5*B*) and was not polyubiquitinated (data not shown), suggesting that PGI/AMF is not degraded via the proteasome system. To examine the effect of PARP-14 suppression on PGI/AMF ubiquitination, siRNA-transfected cells were treated with chloroquine for 5 h at 37°C after transfection, and PGI/AMF ubiquitination was examined. The results clearly show that PARP-14 suppression increased the ubiquitinated PGI/AMF level exhibiting a molecular weight ~8 kDa higher than that of normal (Fig. 5*C*; 2.41 ratio to control). These results reiterate the association between PGI/AMF and PARP-14.

Discussion

In this study, we have identified a cytoplasmic PGI/AMF–interacting protein (i.e., PARP-14). PARP-14 consists of three ADP-ribose-1″ monophosphate processing enzyme (A1pp) domains in the NH_2 terminus and one WWE domain that is named after three of its conserved residues and PARP catalytic domain in the COOH terminus (33). The initial partial sequence of the cloned cDNA of PARP-14 contained WWE and the PARP catalytic domain, but lacked the A1pp domain of the PARP proteins; therefore, we suggest that the COOH terminus of PARP-14 protein that includes these domains are important for the interaction with PGI/AMF.

The proteins containing PARP catalytic domain belongs to the PARP superfamily and thus far 17 different putative PARP homologues were found (34, 35). The PARP domain is located at the COOH terminus of the protein, and is adjacent to various domains that are involved in DNA or RNA binding, protein-protein interactions, or cell signaling (34, 35). The classification of the PARP superfamily can be proposed based on their functional domains or functions: DNA-dependent PARPs (PARP-1 and PARP-2), tankyrases (PARP-5), CCCH-type PARPs (PARP-12, PARP-13, and tiPARP), and macroPARPs (PARP-9, PARP-14, and PARP-15; refs. 34, 35). PARP-1 and PARP-2 are reported to localize in nucleus, bind DNA, be activated by DNA damage, and implicated in DNA repair and maintenance of genomic integrity (36). PARP-1 was also reported to be localized in the mitochondria and suggested to contribute to apoptosis-inducing factor release and cell death (37). PARP-5a (e.g., tankyrase 1) was identified as a binding partner of the human telomere repeat binding factor-1 (TRF1) and its overexpression leads to progressive telomere shortening (38). The poly(ADP-ribosyl)ation of TRF1 by tankyrase 1 releases TRF1 from telomeres, opens up the telomeric complex, allows access to telomerase, and then leads to telomere elongation (38). PARP-5b (tankyrase 2), which exhibits 83% identity to tankyrase 1, behaves like tankyrase 1 in a number of situations; however, it causes caspase-independent cell death through the mitochondrial potential abrogation when overexpressed (39). Tankyrases are distributed throughout the cell compartments and can be found at the telomeres, Golgi complex, nucleus, and nuclear pores (39, 40). PARP-14 belongs to the superfamily of macroPARPs and has two aliases, collaborator of Stat6 (CoaSt6) and B-aggressive lymphoma 2 (BAL2; refs. 41, 42). CoaSt6 interacts with Stat6, which binds to the interleukin 4–inducible CD23 promoter and induces CD23, and amplifies Stat6-mediated gene expression. BAL2 belongs to the BAL family, modulates transcription, and shows the highest transcription level in lymphocyte-rich tissues. The BAL-positive transfectants had ~4-fold higher rates of migration than vector-only transfectants (43).

The results presented here reveal that PARP-14 resides in the cytoplasm and colocalizes with PGI/AMF in the perinuclear region.

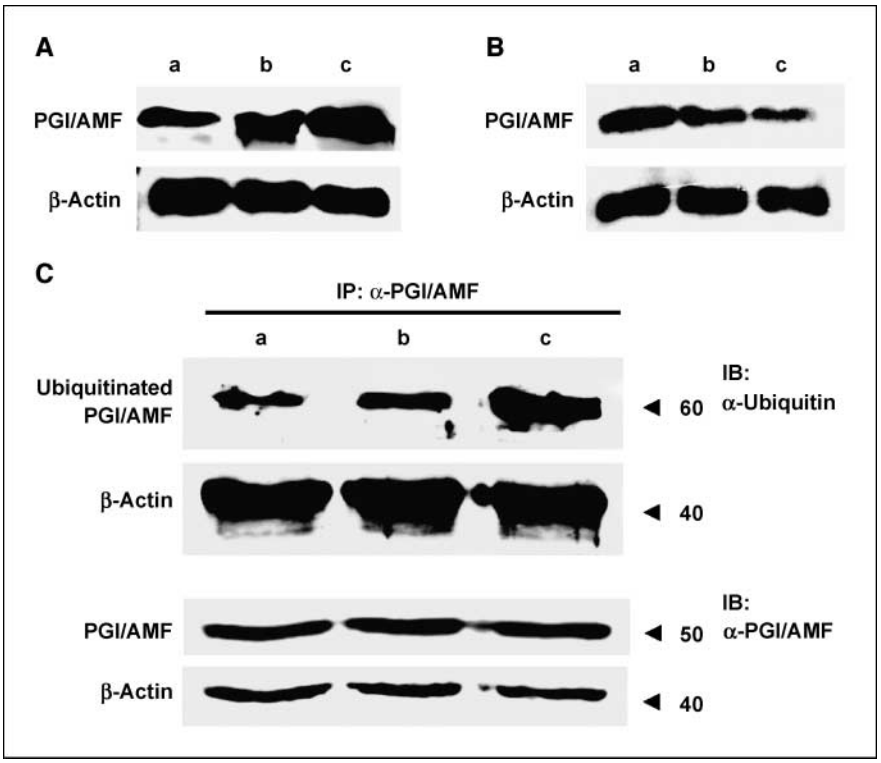

Figure 5. Detection of ubiquitinated PGI/AMF involved with proteasome or lysosome degradation system. *A,* stability of PGI/AMF after treatment with chloroquine or ammonium chloride. The treatment of HT-1080 cells with lysosome inhibitors up-regulated PGI/AMF accumulation. *Lane a,* control; *lane b,* chloroquine treatment; *lane c,* ammonium chloride treatment. *B,* stability of PGI/AMF after treatment with lactacystin or MG132. *Lane a,* control; *lane b,* lactacystin treatment; *lane c,* MG132 treatment. *C,* 2 d after siRNA transfection, transfected cells were treated with chloroquine for 5 h and PGI/AMF ubiquitination was examined. PARP-14 suppression increased ubiquitinated PGI/AMF, the molecular weight of which is ~8 kDa higher than that of the normal one. *Lane a,* cells treated with only LipofectAMINE 2000; *lane b,* cells transfected with GL3 siRNA; *lane c,* cells transfected with PARP-14 siRNA.

PARP-14 suppression by RNA interference comparably reduced the expression of PGI/AMF at the protein level, affecting its function and secretion. However, against our expectation, PARP-14 suppression did not induce down-regulation of cell migration, suggesting that PARP-14 may affect other molecules involved with cell motility or viability. We took into account that aberrant expression of PGI/AMF affects it secretion rate (2, 30) and examined the possibility that PARP-14 may affect the stability of PGI/AMF and subsequently its secretion.

We report that the lysosome inhibitor, chloroquine, induced accumulation and ubiquitination of PGI/AMF, whereas the proteasome inhibitor lactacystin did not, suggesting that PGI/AMF degradation is mainly regulated by the ubiquitin-lysosomal pathway. However, it could be that the resultant change in cytoplasmic pH by chloroquine results in secondary effects on PGI/AMF expression or that changes in acidification affect the atypical secretory pathway that is apparently used by PGI/AMF. Increase of monoubiquitinated PGI/AMF by PARP-14 suppression suggests that PARP-14 regulates the stabilization of PGI/AMF and may subsequently mediate, in part, its secretion that stimulates tumor cell motility and invasion during metastasis. It should be noted that it was recently reported that poly(ADP-ribose) may serve as a signal for protein degradation in oxidative injured cells, although degradation was processed in the proteasome (44, 45). In our study, the fact that malignant tumor cell line HT-1080 cells express more PARP-14 and PGI/AMF than normal Hs68 cells corroborates previous report showing that the level of AMF secretion by tumor cells correlated with the intracellular level of the protein and not with the level of *pgi/amf* transcript, which we may now suggest relates to the level of PARP-14 protein expression inhibiting PGI/AMF degradation and leading to its accumulation and subsequent secretion.

PARP family, which plays a crucial role in DNA damage repair, is also involved in the progression of cancer, because cancer cell proliferation might be unstoppable; however, they still need to repair their DNA as long as they grow. The activity of PARP is extremely high in cancer cells (46). Moreover, PARP activation occurs when cells are damaged in instances such as during chemotherapy or radiotherapy. Targeting PARP may prevent tumor cells from repairing DNA themselves. Cleavage of PARP results in genomic instability, leading to DNA fragmentation and thus to apoptosis in tumor cells (46). In various cancer models, PARP inhibitors have been shown to potentiate the effect of various chemotherapeutic agents (e.g., methylating agents or DNA topoisomerase inhibitors) as well as radiation therapy by increasing apoptosis of cancer cells, limiting tumor growth, decreasing metastasis, and prolonging the survival of tumor-bearing animals (46, 47). In fact, combined treatment with a PARP inhibitor and temozolomide, the DNA-methylating agent, is currently undergoing clinical evaluation (47). One of the well-known properties of cancer cells is increased glycolysis (48, 49). Interestingly, it has been reported that cells using aerobic glycolysis are more susceptible to PARP-1–mediated cell death elicited by DNA-alkylating agents compared with cells catabolizing nonglucose substrates to maintain oxidative phosphorylation (50). Therefore, the expression or the activity of PARP might be connected with glycolysis (i.e., glycolytic enzymes in cancer). Our study here showed one clue that connects PARP with glycolysis, and should be the first report to reveal the interaction between PARP and glycolytic enzyme.

In conclusion, this is the first report detailing that PGI/AMF degradation is regulated via the ubiquitin-lysosome system and not the ubiquitin-proteasome system, and that PARP-14 interaction with PGI/AMF presumably inhibits AMF ubiquitination and enhances its secretion. The identification of PARP-14 regulation of PGI/AMF stability may offer a new therapeutic target aiming at inhibiting cancer cell migration and invasion during metastasis and may further the understanding of the autocrine loop of motile stimulation.

Acknowledgments

Received 4/30/2007; revised 7/9/2007; accepted 7/13/2007.

Grant support: NIH grant CA51714 and Japanese Ministry of Education, Science, Sports and Culture, Grant-in-Aid for Young Scientists (B), 18791033, 2006.

The costs of publication of this article were defrayed in part by the payment of page charges. This article must therefore be hereby marked *advertisement* in accordance with 18 U.S.C. Section 1734 solely to indicate this fact.

We thank V. Powell and V. Hogan for editing the manuscript.

References

1. Harrison RA. The detection of hexokinase, glucosephosphate isomerase and phosphoglucomutase activities in polyacrylamide gels after electrophoresis: a novel method using immobilized glucose 6-phosphate dehydrogenase. Anal Biochem 1974;61:500–7.
2. Funasaka T, Haga A, Raz A, Nagase H. Tumor autocrine motility factor induces hyperpermeability of endothelial and mesothelial cells leading to accumulation of ascites fluid. Biochem Biophys Res Commun 2002;293:192–200.
3. Funasaka T, Haga A, Raz A, Nagase H. Tumor autocrine motility factor is an angiogenic factor that stimulates endothelial cell motility. Biochem Biophys Res Commun 2001;285:118–28.
4. Watanabe H, Takehana K, Date M, Shinozaki T, Raz A. Tumor cell autocrine motility factor is the neuroleukin/phosphohexose isomerase polypeptide. Cancer Res 1996;56:2960–3.
5. Chaput M, Claes V, Portetelle D, et al. The neurotrophic factor neuroleukin is 90% homologous with phosphohexose isomerase. Nature 1988;332:454–5.
6. Xu W, Seiter K, Feldman E, Ahmed T, Chiao JW. The differentiation and maturation mediator for human myeloid leukemia cells shares homology with neuroleukin or phosphoglucose isomerase. Blood 1996;87:4502–6.
7. Yakirevich E, Naot Y. Cloning of a glucose phosphate isomerase/neuroleukin-like sperm antigen involved in sperm agglutination. Biol Reprod 2000;62:1016–23.
8. Cao MJ, Osatomi K, Matsuda R, Ohkubo M, Hara K, Ishihara T. Purification of a novel serine proteinase inhibitor from the skeletal muscle of white croaker (*Argyrosomus argentatus*). Biochem Biophys Res Commun 2000;272:485–9.
9. Matsumoto I, Staub A, Benoist C, Mathis D. Arthritis provoked by linked T and B cell recognition of a glycolytic enzyme. Science 1999;286:1732–5.
10. Takeuchi K, Watanabe H, Takagishi K. Biochemical investigation of cell motile activity in rheumatoid synovial fluid. J Rheumatol 1998;25:9–15.
11. Beutler E, West C, Britton HA, Harris J, Forman L. Glucosephosphate isomerase (GPI) deficiency mutations associated with hereditary nonspherocytic hemolytic anemia (HNSHA). Blood Cells Mol Dis 1997;23:402–9.
12. Schroter W, Eber SW, Bardosi A, Gahr M, Gabriel M, Sitzmann FC. Generalised glucosephosphate isomerase (GPI) deficiency causing haemolytic anaemia, neuromuscular symptoms and impairment of granulocytic function: a new syndrome due to a new stable GPI variant with diminished specific activity (GPI Homburg). Eur J Pediatr 1985;144:301–5.
13. Silletti S, Watanabe H, Hogan V, Nabi IR, Raz A. Purification of B16-1 melanoma autocrine motility factor and its receptor. Cancer Res 1991;51:3507–11.
14. Baumann M, Brand K. Purification and characterization of phosphohexose isomerase from human gastrointestinal carcinoma and its potential relationship to neuroleukin. Cancer Res 1988;48:7018–21.
15. Baumann M, Kappl A, Lang T, Brand K, Siegfried W, Paterok E. The diagnostic validity of the serum tumor marker phosphohexose isomerase (PHI) in patients with gastrointestinal, kidney, and breast cancer. Cancer Invest 1990;8:351–6.
16. Filella X, Molina R, Jo J, Mas E, Ballesta AM. Serum phosphohexose isomerase activities in patients with colorectal cancer. Tumour Biol 1991;12:360–7.
17. Yanagawa T, Funasaka T, Tsutsumi S, Raz T, Tanaka N, Raz A. Differential regulation of phosphoglucose isomerase/autocrine motility factor activities by protein kinase CK2 phosphorylation. J Biol Chem 2005;280:10419–26.
18. Yanagawa T, Watanabe H, Takeuchi T, Fujimoto S,

Kurihara H, Takagishi K. Overexpression of autocrine motility factor in metastatic tumor cells: possible association with augmented expression of KIF3A and GDI-β. Lab Invest 2004;84:513–22.
19. Tsutsumi S, Yanagawa T, Shimura T, Kuwano H, Raz A. Autocrine motility factor signaling enhances pancreatic cancer metastasis. Clin Cancer Res 2004;10:7775–84.
20. Shimizu K, Tani M, Watanabe H, et al. The autocrine motility factor receptor gene encodes a novel type of seven transmembrane protein. FEBS Lett 1999;456:295–300.
21. Fang S, Ferrone M, Yang C, Jensen JP, Tiwari S, Weissman AM. The tumor autocrine motility factor receptor, gp78, is a ubiquitin protein ligase implicated in degradation from the endoplasmic reticulum. Proc Natl Acad Sci U S A 2001;98:14422–7.
22. Chen B, Mariano J, Tsai YC, Chan AH, Cohen M, Weissman AM. The activity of a human endoplasmic reticulum-associated degradation E3, gp78, requires its Cue domain, RING finger, and an E2-binding site. Proc Natl Acad Sci U S A 2006;103:341–6.
23. Li G, Zhou X, Zhao G, Schindelin H, Lennarz WJ. Multiple modes of interaction of the deglycosylation enzyme, mouse peptide *N*-glycanase, with the proteasome. Proc Natl Acad Sci U S A 2005;102:15809–14.
24. Mishra S, Raz A, Murphy LJ. Insulin-like growth factor binding protein-3 interacts with autocrine motility factor/phosphoglucose isomerase (AMF/PGI) and inhibits the AMF/PGI function. Cancer Res 2004;64:2516–22.
25. Talukder AH, Bagheri-Yarmand R, Williams RR, Ragoussis J, Kumar R, Raz A. Antihuman epidermal growth factor receptor 2 antibody herceptin inhibits autocrine motility factor (AMF) expression and potentiates antitumor effects of AMF inhibitors. Clin Cancer Res 2002;8:3285–9.
26. Cohen S, Knoll BJ, Little JW, Mount DW. Preferential cleavage of phage λ repressor monomers by recA protease. Nature 1981;294:182–4.
27. Colicelli J, Birchmeier C, Michaeli T, O'Neill K, Riggs M, Wigler M. Isolation and characterization of a mammalian gene encoding a high-affinity cAMP phosphodiesterase. Proc Natl Acad Sci U S A 1989;86:3599–603.
28. Elbashir SM, Harborth J, Lendeckel W, Yalcin A, Weber K, Tuschl T. Duplexes of 21-nucleotide RNAs mediate RNA interference in cultured mammalian cells. Nature 2001;411:494–8.
29. Gracy RW, Tilley BE. Phosphoglucose isomerase of human erythrocytes and cardiac tissue. Methods Enzymol 1975;41:392–400.
30. Tsutsumi S, Hogan V, Nabi IR, Raz A. Overexpression of the autocrine motility factor/phosphoglucose isomerase induces transformation and survival of NIH-3T3 fibroblasts. Cancer Res 2003;63:242–9.
31. Thrower JS, Hoffman L, Rechsteiner M, Pickart CM. Recognition of the polyubiquitin proteolytic signal. EMBO J 2000;19:94–102.
32. Hicke L. Protein regulation by monoubiquitin. Nat Rev Mol Cell Biol 2001;2:195–201.
33. Aravind L. The WWE domain: a common interaction module in protein ubiquitination and ADP ribosylation. Trends Biochem Sci 2001;26:273–5.
34. Schreiber V, Dantzer F, Ame JC, de Murcia G. Poly(ADP-ribose): novel functions for an old molecule. Nat Rev Mol Cell Biol 2006;7:517–28.
35. Ame JC, Spenlehauer C, de Murcia G. The PARP superfamily. BioEssays 2004;26:882–93.
36. Nguewa PA, Fuertes MA, Valladares B, Alonso C, Perez JM. Poly(ADP-ribose) polymerases: homology, structural domains and functions. Novel therapeutical applications. Prog Biophys Mol Biol 2005;88:143–72.
37. Du L, Zhang X, Han YY, et al. Intra-mitochondrial poly(ADP-ribosylation) contributes to NAD+ depletion and cell death induced by oxidative stress. J Biol Chem 2003;278:18426–33.
38. Smith S, de Lange T. Tankyrase promotes telomere elongation in human cells. Curr Biol 2000;10:1299–302.
39. Kaminker PG, Kim SH, Taylor RD, et al. TANK2, a new TRF1-associated poly(ADP-ribose) polymerase, causes rapid induction of cell death upon overexpression. J Biol Chem 2001;276:35891–9.
40. Smith S, Giriat I, Schmitt A, de Lange T. Tankyrase, a poly(ADP-ribose) polymerase at human telomeres. Science 1998;282:1484–7.
41. Goenka S, Boothby M. Selective potentiation of Stat-dependent gene expression by collaborator of Stat6 (CoaSt6), a transcriptional cofactor. Proc Natl Acad Sci U S A 2006;103:4210–5.
42. Aguiar RC, Takeyama K, He C, Kreinbrink K, Shipp MA. B-aggressive lymphoma family proteins have unique domains that modulate transcription and exhibit poly(ADP-ribose) polymerase activity. J Biol Chem 2005;280:33756–65.
43. Aguiar RC, Yakushijin Y, Kharbanda S, Salgia R, Fletcher JA, Shipp MA. BAL is a novel risk-related gene in diffuse large B-cell lymphomas that enhances cellular migration. Blood 2000;96:4328–34.
44. Ciftci O, Ullrich O, Schmidt CA, Diestel A, Hass R. Regulation of the nuclear proteasome activity in myelomonocytic human leukemia cells after Adriamycin treatment. Blood 2001;97:2830–8.
45. Ullrich O, Grune T. Proteasomal degradation of oxidatively damaged endogenous histones in K562 human leukemic cells. Free Radic Biol Med 2001;31:887–93.
46. Virag L, Szabo C. The therapeutic potential of poly(ADP-ribose) polymerase inhibitors. Pharmacol Rev 2002;54:375–429.
47. Jagtap P, Szabo C. Poly(ADP-ribose) polymerase and the therapeutic effects of its inhibitors. Nat Rev Drug Discov 2005;4:421–40.
48. Pelicano H, Martin DS, Xu RH, Huang P. Glycolysis inhibition for anticancer treatment. Oncogene 2006;25:4633–46.
49. Warburg O. On the origin of cancer cells. Science 1956;123:309–14.
50. Zong WX, Ditsworth D, Bauer DE, Wang ZQ, Thompson CB. Alkylating DNA damage stimulates a regulated form of necrotic cell death. Genes Dev 2004;18:1272–82.

Regulation of Phosphoglucose Isomerase/Autocrine Motility Factor Activities by the Poly(ADP-Ribose) Polymerase Family-14

Takashi Yanagawa, Tatsuyoshi Funasaka, Soichi Tsutsumi, et al.

Cancer Res 2007;67:8682-8689.